A MAGNET LATTICE FOR THE LNLS UV SYNCHROTRON LIGHT SOURCE

L.Lin, L.Jahnel and P.Tavares
LNLS - Laboratório Nacional de Luz Síncrotron
Cx. Postal 6192 - Campinas - SP - Brazil

Abstract

The Brazilian Synchrotron Light Laboratory (LNLS) [1] is designing and building an electron storage ring for the production of VUV and soft X-ray photons (λ_c = 10 Å from the bending magnets). This paper describes a proposal for the magnet lattice of this machine, including studies of sensitivity to alignment and multipole errors, dynamic aperture and collective effects.

1 Introduction

The design of a storage ring dedicated to the production of synchrotron radiation has to meet several requirements including performance specifications (determined by the users) and technological and cost constraints. The many options that are available to the designer, such as the choice of the lattice and the periodicity of the ring, influence strongly both requirements. Therefore, several candidate designs have to be analysed. The proposal presented here (*UVX1*) is the latest in the series of alternative designs being considered by LNLS.

The main requirements for the VUV-Soft X-Ray electron storage ring are:

- The critical photon wavelength from the bending magnets should be 10 Å.
- The lattice should include long straight sections to accomodate insertion devices, specially wigglers to produce harder photons.
- A long electron beam lifetime of the order of 10 hours is to be achieved.
- The design of the bending magnets should be conservative.
- It is of paramount importance that the operation of the ring should be reliable. This includes low sensitivity of the lattice to errors and flexibility enough to allow for other operation modes (specially high emittance modes interesting during commissioning), correction of insertion devices effects, etc.
- Feasible low energy (100-200 MeV) injection. The injector adopted is a SLAC type electron Linac.
- Small number of magnetic elements

2 Magnet Lattice

The proposed solution *UVX1* is a six fold symmetric double-bend Chasman-Green achromat lattice. See figure 1. It has twelve 1.4 Tesla rectangular bending magnets [2]. The energy of the ring is 1.15 GeV providing λ_c = 10 Å. The achromats connect six 3-meter long dispersion free straight sections, four of which allow for insertion devices (one is used for injection and another for the RF cavity).

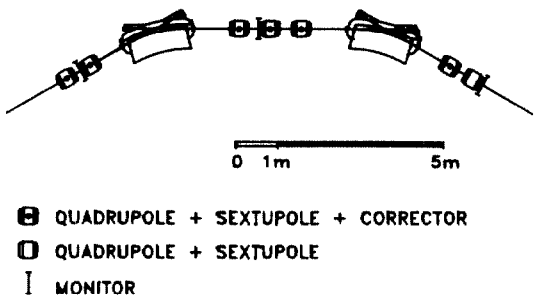

Figure 1: Lay-out of one superperiod of 1.15 GeV *UVX1* storage ring.

	UVX1	*UVX1-H*	*UVX1-L*	
Energy		1.15		GeV
Current		100		mA
Circumference		77.34		m
Magnetic structure		Chasman-Green , 6-fold symmetric		
Revolution frequency		3876.05		kHz
Harmonic number		129		
RF-frequency		500.		MHz
Natural emittance	63.	115.	33.	nm.rad
Horizontal betatron tune	5.23	4.75	5.72	
Vertical betatron tune	2.12	1.82	2.81	
Synchrotron tune		4.054		(1/1000)
Momentum compaction factor		0.010		
Natural energy spread		0.059		%
Nat. horiz. chromaticity	-8.3	-5.4	-21.2	
Nat. vert. chromaticity	-6.2	-5.5	-5.7	
Horiz. betatron damping time		11.0		ms
Vert. betatron damping time		10.5		ms
Synchrotron damping time		5.1		ms
Dipoles				
Bending radius		2.735		m
Bending field		1.4		Tesla
Number		12		
Quadrupoles				
Max. gradient	3.6	4.0	4.1	m^{-2}
Number of families		4		
Number of quadrupoles		42		
Sextupoles				
Max. int. strength*	6.7	3.6	5.1	m^{-2}
Number of families		4		
Number of sextupoles		42		
Injection energy		100		MeV

*Values for zero chromaticity

Table 1: Main parameters of the *UVX1* storage ring.

The double-bend achromatic arc consists of two 30 degree bending magnets separated by one vertically focusing and two horizontally focusing quadrupoles. The chromaticity correction sextupolar fields are achieved with additional coils inside these quadrupoles. This is the same scheme adopted for Super-Aco [3] .

Two additional operating modes (a higher emittance (*UVX1-H*) and a lower emittance (*UVX1-L*) mode) are being investigated and are at different stages of study.

The main parameters of *UVX1* are listed in table 1 . Figure 2 shows the optical functions for one superperiod.

Besides the two sextupole families for chromaticity correction, two other families in the non-dispersive section were used to compensate for the geometric aberration produced by the chromatic sextupoles. This can be done at almost no extra cost since the quadrupoles are already designed to allow for sextupolar coils.

Figure 3 shows the tune dependence on particle momentum.

All calculations described here are done with the following computer codes:

- MAD [4] - for linear lattice optimization.
- PATPET [5] - for chromaticity correction, tracking with multipoles, magnet imperfections, orbit distortions, tracking with energy oscillations and orbit correction.

2.1 Sensitivity to Errors and Dynamic Aperture

Dynamic aperture studies were performed with the code PATPET. Particles were tracked for 500 turns for various situations:

- without errors,
- with systematic multipole errors,

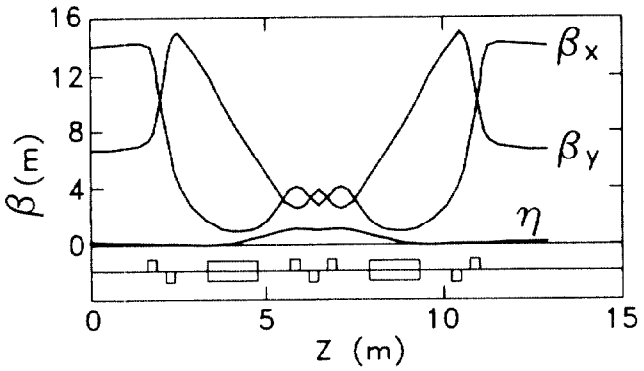

Figure 2: Optical functions along one superperiod for *UVX1* .

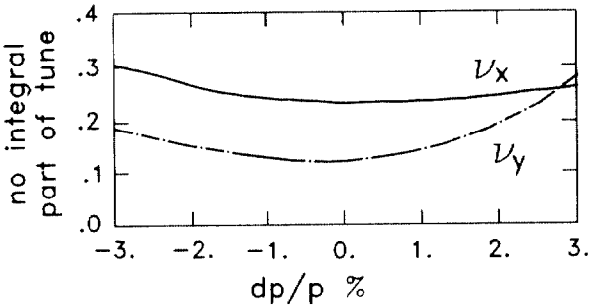

Figure 3: Tune variation with particle momentum.

- with random multipole errors,
- with random excitation errors,
- with random alignment errors, and
- with momentum deviation.

The values of systematic and random multipole errors used are given in table 2. The alignment errors considered are horizontal $< x >$ and vertical $< y >$ displacements and rotation $< \alpha >$ about the longitudinal axis. The values used are given in table 3. All tabulated random errors are r.m.s values for a gaussian distribution truncated at two sigmas.

$$B(x) = B\rho \sum_n \frac{k_n x^n}{n!} = \sum_n B_n$$

n	Dipole B_n/B_o*		Quadrupole B_n/B_1*	
	Systematic	Random	Systematic	Random
0	-	5×10^{-5}	-	1×10^{-3}
1	2×10^{-5}	1×10^{-4}	-	5×10^{-4}
2	-	2×10^{-5}	-	2×10^{-4}
3	2×10^{-6}	1×10^{-5}	-	6×10^{-5}
5	-	-	1×10^{-4}	1×10^{-5}
9	-	-	1×10^{-9}	1×10^{-8}

* Values at x = 1 cm.

Table 2: Magnetic multipole errors.

For the cases where excitation and alignment errors are included, tracking is done after closed orbit corrections. Some of the results are shown in figures 4 and 5. The hatched region in figure 5 correspond to the maximum and minimum limits of stable particle motion for five sets of random errors used.

$< \Delta x >=$	0.2 mm
$< \Delta y >=$	0.2 mm
$< \Delta \alpha >=$	0.02^o
$< \Delta S/S >=$	0.01%

Table 3: Alignment and Strength Random Errors in Magnetic Elements.

2.2 Closed Orbit Distortion and Correction

For the closed orbit correction 18 monitors for both horizontal and vertical readings, 18 horizontal and 12 vertical correctors are used. The correctors are placed inside the quadrupoles. Figure 1 shows the distribution of these elements in one superperiod.

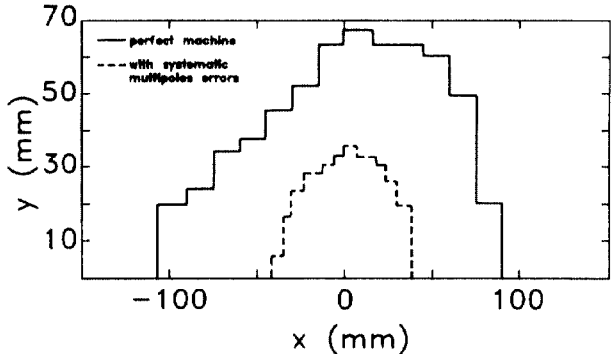

Figure 4: Dynamic aperture for the perfect machine and with systematic multipole errors only.

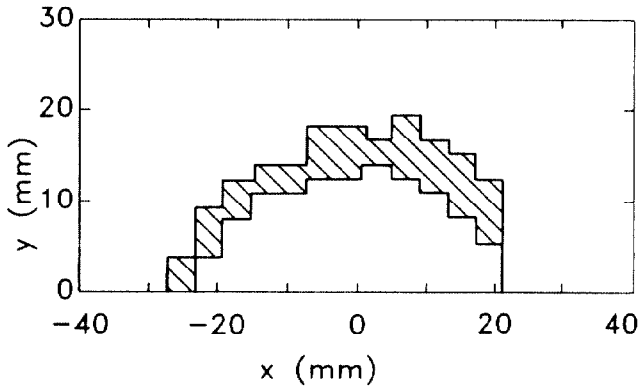

Figure 5: Dynamic aperture with systematic and random errors, strength and alignment errors and without momentum deviation.

The algorithm used for the orbit correction minimizes the r.m.s. values of the monitor readings. Five correction iterations are used.

Ten random machines are studied for the nominal errors given in table 3. In table 4 we give the average and standard deviation of various parameters before and after correction.

Parameter	Unperturbed machine	Perturbed machine	Corrected machine
ν_x	5.233	5.237 ± 0.006	5.237 ± 0.002
ν_y	2.119	2.124 ± 0.005	2.122 ± 0.003
$< x^2 >^{1/2}$(mm)	0.0	1.9 ± 0.9	0.17 ± 0.05
x_{max}(mm)	0.0	4.5 ± 2.0	0.6 ± 0.2
$< y^2 >^{1/2}$(mm)	0.0	3.4 ± 1.1	0.06 ± 0.01
y_{max}(mm)	0.0	$7.6 + 2.4$	$0.19 + 0.06$
$< \eta_x^2 >^{1/2}$(cm)	40.4	40.6 ± 0.2	40.4 ± 0.2
$< \eta_y^2 >^{1/2}$(cm)	0.0	5.5 ± 3.2	2.0 ± 1.2
$\epsilon_x(10^{-9}$rad.m)	63.3	69.1 ± 10.9	65.8 ± 3.7
$\epsilon_y(10^{-9}$rad.m)	0.0	0.6 ± 0.5	0.10 ± 0.11
ϵ_y/ϵ_x(%)	0.0	0.8 ± 0.5	0.15 ± 0.18
$< \theta_x >$ (mrad)	-	-	0.15 ± 0.04
$< \theta_{x,max} >$ (mrad)	-	-	0.41 ± 0.16
$< \theta_y >$ (mrad)	-	-	0.10 ± 0.02
$< \theta_{y,max} >$ (mrad)	-	-	0.25 ± 0.05

Table 4: Closed orbit correction. Comparison between unperturbed, perturbed and corrected machines.

3 Collective Effects and Beam Lifetime

Collective effects are especially important for *UVX1* because a low energy (100 MeV) injection scheme is envisaged. Beam lifetimes at low energy should therefore be long enough to allow accumulation of the design ring current (400 mA).

In what follows, we shall be concerned with the following issues

- microwave instability (turbulent bunch lengthening) and potential well distortion,

- emittance growth due to intra-beam scattering (IBS),
- beam lifetime.

It is important to notice that these questions are correlated. Touschek lifetime, for example, depends on bunch density, which in turn depends on the equilibrium emittance and bunch length determined by IBS and microwave instability. A calculation that takes all these effects into account consistently is done with the LBL accelerator physics code ZAP [6]. All calculations are done for 100 MeV (injection energy) and 1.15 GeV assuming a 500 MHz RF system. Thresholds for single bunch instabilities depend on the broadband impedance of the ring. Both the higher order modes (HOM) of the RF cavities and the ring vacuum chamber descontinuities contribute to the broadband impedance. Ideally, one would have to measure the broadband impedance and HOM of the accelerating cavities. However, at the present stage, neither measurements nor calculations are available and we resort to the literature for typical values. For the ring impedance we use 13 Ω (value measured at Alladin [7]) and 2 Ω (measured at Super-Aco [8]) Although the value measured at Alladin is considerably higher than those reported for other rings, we feel it is advisable to have a worst case estimate of single bunch thresholds. However, a high impedance does not necessarily imply a poor Touschek lifetime, hence the calculations with the 2 Ω impedance. The assumed frequency dependence of the broadband impedance is that of a Q = 1 resonator, centred at the beam pipe cut-off frequency. The phenomenological SPEAR scaling law is used to get an effective impedance for short bunches.

3.1 Bunch lengthening

The equilibrium bunch length, and momentum spread as determined by the combined effects of microwave instability and potential well distortion is shown in figure 6 for 100 MeV and 1.15 GeV. The microwave instability threshold is considerably higher at 1.15 GeV than at 100 Mev.This is why one observes bunch shortening (due to potential-well distortion) which is not accompanied by any change in energy dispersion for currents below the threshold.

3.2 Intra-Beam Scattering

At 100 MeV, multiple small-angle Coulomb scattering within a bunch causes the beam emittance to grow.

Figure 7 shows the equilibrium emittance as determined by IBS at 100 MeV for various average currents in a single bunch as a function of the RF peak voltage. No emittance blow-up due to IBS is observed at 1.15 GeV.

3.3 Lifetime

Three beam lifetime limiting processes are considered: Touschek scattering, elastic and inelastic (Bremsstrahlung) scattering from the nuclei of residual gas molecules. Touschek lifetime and Bremsstrahlung lifetime depend strongly on the momentum acceptance of the ring. This can be determined by the RF system or by the lattice. For *UVX1* at 1.15 GeV, the momentum acceptance is determined by the RF bucket (1.96% at 1 MV peak RF voltage). Whereas at 100 MeV it is determined by the lattice (2.48% averaged over the lattice for 600 MV peak RF voltage).

Elastic scattering lifetime depends on the betatron acceptance of the ring which can be determined by the physical or dynamic aperture. For *UVX1* the dynamic aperture is the limiting factor.

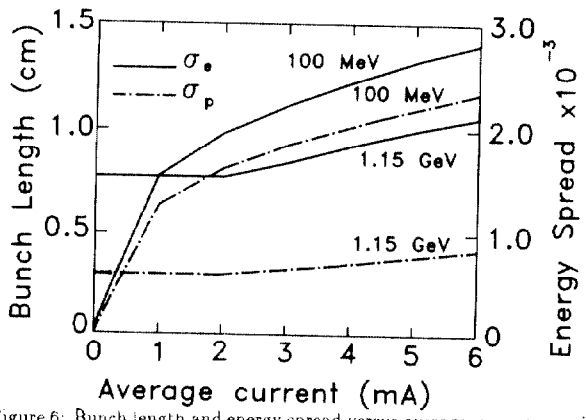

Figure 6: Bunch length and energy spread versus average current in a single bunch. Broadband impedance is 2 Ω (no SPEAR scaling). Peak RF voltage is 200 KV at 100 MeV and 500 KV at 1.15 GeV.

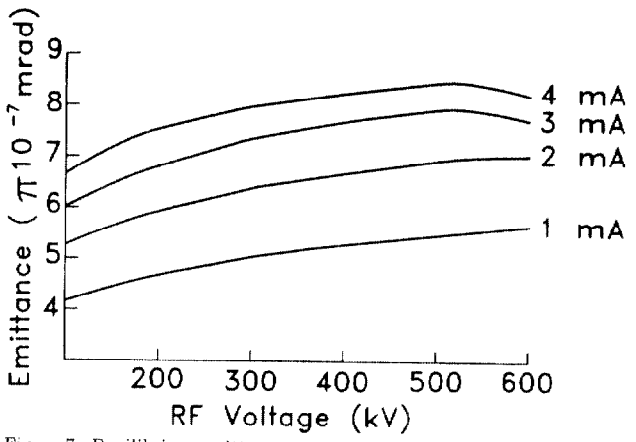

Figure 7: Equilibrium emittance versus RF peak voltage at 100 MeV for various average currents in a single bunch. Broadband impedance is 2 Ω (no SPEAR scaling).

Gas scattering lifetimes are calculated assuming a 1nT pressure. This gives a total gas scattering lifetime of 36 hours at 1.15 GeV and 42.0 minutes at 100 MeV.

Although Touschek lifetime decreases sharply with energy, the concomitant emittance blow up due to IBS decreases the bunch density significantly so that an acceptable Touschek lifetime can be achieved at 100 MeV (figure 8). Beam lifetime at 100 MeV is therefore limited by scattering from residual gas molecules. At 1.15 GeV, Touschek lifetime is limited by the momentum acceptance of the RF system.

Further investigation of collective effects in *UVX1* is under way. Single bunch transverse instabilities (which determine the maximum current that can be stored in the ring) and ion trapping (which has caused problems in other electron machines with low energy injection schemes) are the main topics.

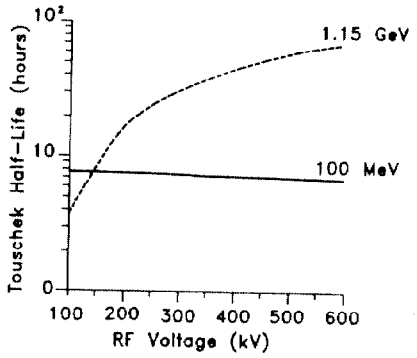

Figure 8: Touschek half-life at 100 MeV. Single bunch average current is 4 mA. Broadband impedance is 13 Ω (no SPEAR scaling).

References

[1] C.E.T.Gonçalves da Silva, A.R.D.Rodrigues and D.Wisnivesky, 'LNLS: The Brazilian Synchrotron Light Laboratory',presented at IEEE PAC, Chicago, 1989.

[2] F.W.B.Talarico and R.T.Neuenschwander, 'Dipole Magnet for the LNLS Synchrotron Light Source', presented at this conference.

[3] A.Dael et. al., 'Magnet System for the SUPER ACO - The New Orsay Radiation Source', presented at the 9^{th} International Conference on Magnet Technology (1985)

[4] F.C.Iselin and J.Niederer, 'The MAD Program', CERN/LEP-TH/88-38.

[5] L.Emery, H.Wiedemann and J.Safranek, 'Users's Guide for PATPET Version 88.2', SSRL ACD-NOTE 36.

[6] M.S.Zisman, S.Chattopadhyay and J.J.Bisognano, 'ZAP Users's Manual', LBL - 21270 (1986).

[7] S.Chattopadhyay, M.Cornacchia, A.Jackson and M.S.Zisman, 'Accelerator Physics Experiments at Alladin', LBL.

[8] P.Marin and S.Souchet, 'Vacuum Chamber and Related Problems', Super Aco Internal Report Anneau/RT/88-03.